



# Microvascular flow imaging to differentiate focal hepatic lesions: the spoke-wheel pattern as a specific sign of focal nodular hyperplasia

## ULTRASONOGRAPHY

Aladár Dávid Rónaszéki<sup>1</sup>, Ibolyka Dudás<sup>1</sup>, Boglárka Zsély<sup>1</sup>, Bettina Katalin Budai<sup>1</sup>, Róbert Stollmayer<sup>1</sup>, Oszkár Háhn<sup>2</sup>, Barbara Csongrády<sup>1</sup>, Byung-so Park<sup>3</sup>, Pál Maurovich-Horvat<sup>1</sup>, Gabriella Györi<sup>1</sup>, Pál Novák Kaposi<sup>1</sup>

<sup>1</sup>Department of Radiology, Medical Imaging Centre, Faculty of Medicine, Semmelweis University, Budapest, Hungary; <sup>2</sup>Department of Surgery, Transplantation and Gastroenterology, Faculty of Medicine, Semmelweis University, Budapest, Hungary; <sup>3</sup>Medical Affairs Manager at Samsung Medison, Samsung Medison Co., Ltd., An Affiliate of Samsung Electronics, Seoul, Korea

Microvascular flow imaging (MVFI) is an advanced Doppler ultrasound technique designed to detect slow-velocity blood flow in small-caliber microvessels. This technique is capable of real-time, highly detailed visualization of tumor vessels without using a contrast agent. MVFI has been recently applied for the characterization of focal liver lesions and has revealed typical vascularity distributions in multiple types thereof. Focal nodular hyperplasia (FNH) constitutes an important differential diagnosis of malignant liver tumors. In this essay, we provide iconographic documentation of the MVFI appearance of FNH and other common solid liver lesions. Identifying the typical patterns of vascularity, including the spoke-wheel pattern with MVFI, can expedite the diagnosis, spare patients from unnecessary procedures, and save costs.

**Keywords:** Focal nodular hyperplasia; Microvascular Doppler ultrasound; Focal liver lesion; Diagnostic sign

**Key points:** Microvascular flow imaging (MVFI) is an advanced Doppler ultrasound technique specifically designed to detect slow-velocity blood flow in microvessels. The spoke-wheel vascularity pattern is characteristic of focal nodular hyperplasia, which has been consistently detected with MVFI. Doing so can expedite the diagnosis, spare patients from unnecessary procedures, and save costs.

### Introduction

Ultrasonography (US) is now becoming the first-line imaging modality to screen, characterize, and follow up focal liver lesions (FLLs). US is a highly accessible, cost-effective, non-ionizing imaging

### PICTORIAL ESSAY

<https://doi.org/10.14366/usg.22028>  
eISSN: 2288-5943  
Ultrasonography 2023;42:172-181

Received: February 18, 2022  
Revised: July 6, 2022  
Accepted: July 9, 2022

#### Correspondence to:

Pál Novák Kaposi, MD, PhD,  
Department of Radiology, Medical  
Imaging Centre, Faculty of Medicine,  
Semmelweis University, Korányi Sándor  
str. 2., H-1083 Budapest, Hungary  
Tel. +36-1-459-1500/61628  
Fax. +36-1-459-1500/61626  
E-mail: [kaposi.pal@med.semmelweis-univ.hu](mailto:kaposi.pal@med.semmelweis-univ.hu)

This is an Open Access article distributed under the terms of the Creative Commons Attribution Non-Commercial License (<http://creativecommons.org/licenses/by-nc/4.0/>) which permits unrestricted non-commercial use, distribution, and reproduction in any medium, provided the original work is properly cited.

Copyright © 2023 Korean Society of  
Ultrasound in Medicine (KSUM)



#### How to cite this article:

Rónaszéki AD, Dudás I, Zsély B, Budai BK, Stollmayer R, Háhn O, et al. Microvascular flow imaging to differentiate focal hepatic lesions: the spoke-wheel pattern as a specific sign of focal nodular hyperplasia. *Ultrasonography*. 2023 Jan;42(1):172-181.

modality used to investigate suspected liver diseases and follow up patients with malignancies. Over 50% of incidentally detected FLLs do not allow a conclusive diagnosis; inconclusive US scans often lead to further imaging studies such as dynamic contrast-enhanced computed tomography (CT) and hepatocyte-specific contrast-enhanced magnetic resonance imaging (MRI) [1] or invasive procedures, such as liver biopsy [2,3]. Therefore, there is a growing demand for novel multi-parametric imaging techniques facilitating the diagnosis of benign and malignant tumors. Contrast-enhanced US (CEUS) for FLLs is becoming a more cost-effective alternative to CT and MRI [4]. The detection of unique vascularity patterns and contrast enhancement dynamics with US can significantly improve the characterization of FLLs.

## Ultrasound-Based Microvascular Flow Imaging

Microvascular flow imaging (MVFI) is an advanced Doppler ultrasound technique to visualize slow-velocity flow in small-caliber vessels [5]. Conventional color Doppler imaging (CDI) uses a temporally constant wall filter to suppress low-frequency noise caused by cardiac pulsations, tissue vibrations, and patient movements. However, there is an overlap between the frequency ranges of low-velocity flow and tissue clutter. Conventional one-dimensional wall filters eliminate low-frequency signals from both sources, making it impossible to detect small-caliber vessels with CDI. Meanwhile, MVFI uses advanced multi-directional filters, which can separate microvascular flow from tissue clutter by analyzing the signal's spatiotemporal coherence. The advantages of MVFI include its ability to visualize low-velocity flow with high spatial resolution for the analysis of microvessel architecture [6]. MVFI has tumor type-specific vascular patterns for the characterization of FLLs, according to recent studies [7]. A spoke-wheel distribution of vascularity, similar to the one detected during the wash-in phase with CEUS, has been consistently identified in focal nodular hyperplasia (FNH) using MVFI; and this pattern has been proposed as a potential new diagnostic sign [8]. This essay aims to demonstrate the excellent discernibility of the spoke-wheel pattern with MVFI. We also provide some examples of the typical MVFI appearances of various FLLs.

### Imaging Technique

In this paper, we present nine patients with different types of FLLs characterized with conventional US and MVFI. Table 1 provides a summary of the imaging studies and other procedures used for the diagnosis of the cases presented in this essay. During the US examination, an expert radiologist scanned each patient after 4 hours of fasting in a supine position with arms overhead, using

a Samsung RS85 Prestige (Samsung Medison Co., Ltd., Seoul, Korea) scanner with a CA1-7S convex probe. First, the lesions were visualized and characterized in B-mode, including their localization, size, shape, and echogenicity. Next, either CDI or directional power Doppler imaging (PDI) with the S-Flow application was used for the initial assessment of the vascularity [5,7,9]. The conventional Doppler scans were performed with a low pulse repetition frequency (typically 0.32 kHz to 1.16 kHz for CDI, and 0.20 kHz to 0.99 kHz for PDI) and power setting (typically 70 to 90 for both) to maximize the flow signal until the noise did not cause spillover. To detect the microvessel distribution inside the lesions we performed MVFI with the MV-Flow application using the same abdominal probe. In the general abdominal presets, the flow-velocity scale was automatically set between  $-2.3$  cm/s and  $2.3$  cm/s; and the flow intensity was displayed on a monochromatic color scale using the power mode of the application. A hand-selected Doppler window was applied to cover the lesion in a split-screen imaging mode (B-mode and MVFI). The acquisition parameters were set to provide an optimal flow signal in the region of the examined FLL; the typical settings were a frame average of 5 to 7, a tissue suppression of 2 to 3, a filter of 2 to 3, a sensitivity of 26 to 32, a dynamic range of 25 to 35, a balance of 20 to 30 and a power of 80 to 90. Patients were instructed to hold their breath during the MVFI acquisitions, and short videos were recorded while the entire lesion was scanned with slow fanning of the probe along the short axis. The vascularity patterns of the lesions were determined based on the previously published classification system of Lee et al. [5] (Fig. 1).

### MVFI Findings of FNH

FNH is the second most common benign solid liver lesion. The most likely pathogenesis of FNH is hyperplastic proliferation of hepatocytes due to an arterial malformation. Typically, FNH is an incidental finding, most commonly detected in young women, and seldom requires any treatment except regular follow-up. The clinical significance of FNH comes from its differential diagnoses, which include hypervascular liver tumors such as hepatocellular carcinoma (HCC). In contrast to the uniformly hyperechoic appearance of typical hemangiomas, the echogenicity of FNHs can vary from isoechoic (Fig. 2) to hyperechoic (Fig. 3) and hypoechoic (Figs. 4, 5) [10]. It can be difficult to delineate the contours of an isoechoic FNH with US, and occasionally only the mass effect causing dislocation or compression of hepatic vessels is visible. Pulsatile central color signals corresponding to a feeding artery and a spoke-wheel vascular pattern are well-documented findings with CDI or PDI in FNH (Figs. 4, 5) [11]. Unfortunately, these helpful diagnostic signs are only visible in a minority of lesions using CDI because the

**Table 1.** Vascular architecture patterns of the nine focal liver lesions that were evaluated with microvascular flow imaging in comparison with the results of CEUS, CT, and MRI findings

Patient No.	Age (year)	Sex	Diagnosis	MVFI pattern <sup>a)</sup>	Echogenicity	CEUS	Wash-in CEUS pattern <sup>a)</sup>	Other diagnostic methods
1	31	F	FNH	Spoke-wheel	Isoechoic	Yes	Spoke-wheel	DCE-CT
2	33	F	FNH	Spoke-wheel	Hyperechoic	Yes	Spoke-wheel	–
3	43	F	FNH	Spoke-wheel	Hypoechoic	Yes	Central feeding artery	HSC-MRI
4	23	M	FNH	Spoke-wheel	Hypoechoic	Yes	Spoke-wheel	–
5	30	F	Hemangioma	Spotty dot-like	Hyperechoic	No	–	Follow-up US
6	70	M	Hemangiomatosis	Nodular rim with a dot-like pattern	Hypoechoic	No	–	CE-MRI
7	80	F	Metastasis	Hypovascular center with vascular rim	Hyperechoic	No	–	DCE-CT, biopsy
8	69	F	Metastasis	Basket weave	Isoechoic	No	–	DCE-CT, biopsy
9	78	M	HCC	Non-specific hypervascular	Mixed echogenicity	No	–	HSC-MRI, biopsy

CEUS, contrast-enhanced ultrasonography; CT, computed tomography; MRI, magnetic resonance imaging; MVFI, microvascular flow imaging; F, female; FNH, focal nodular hyperplasia; DCE-CT, dynamic contrast-enhanced computed tomography; HSC-MRI, hepatocyte-specific contrast-enhanced magnetic resonance imaging; M, male; US, ultrasonography; CE-MRI, contrast-enhanced magnetic resonance imaging; HCC, hepatocellular carcinoma.

<sup>a)</sup>The six categories of microvascular imaging patterns detected in this case series are defined in Fig. 1 based on the classification system of Lee et al. [5].

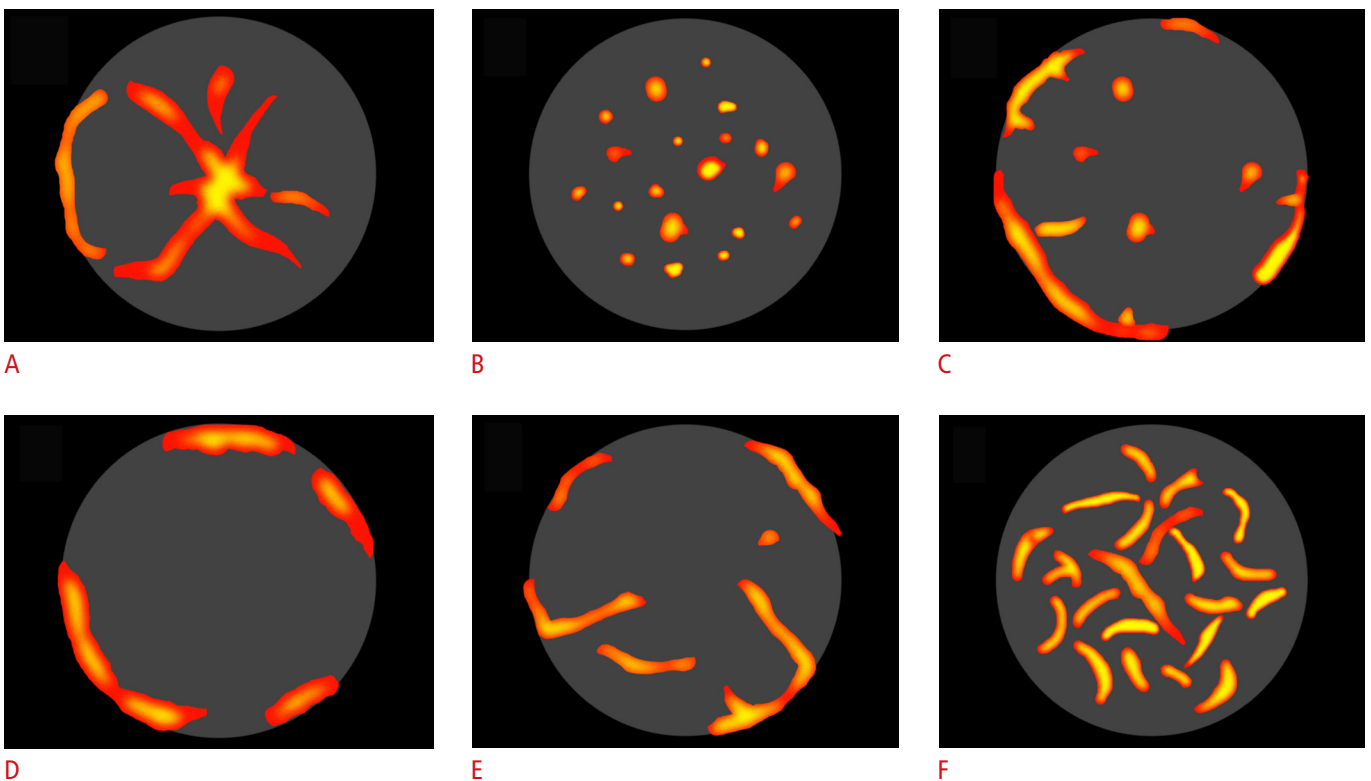


**Fig. 1.** Patterns of vascularization assessed by microvascular flow imaging.

The figures illustrate six different microvascular imaging patterns of focal liver lesions detected in this case series defined according to Lee et al. [5]: spoke-wheel pattern (A), spotty dot-like pattern (B), nodular rim with a dot-like pattern (C), hypovascular center with marginal vessels pattern (D), non-specific hypervascular pattern (E), and basket weave pattern (F).

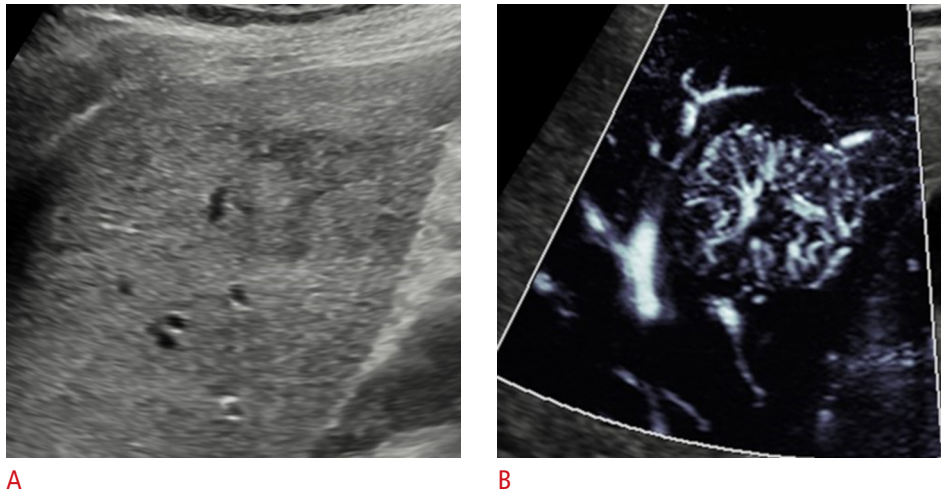


**Fig. 2.** A 31-year-old woman with focal nodular hyperplasia. Microvascular flow imaging (MVFI) shows a spoke-wheel vascular pattern (patient 1). **A.** A poorly circum-scribed isoechoic focal lesion was identified in segment V. of the liver with grayscale ultrasonography in a patient without known malignancy. **B.** The MVFI assessment visualizes a spoke-wheel vascular pattern consisting of microvessels circumferentially radiating out from the center of the lesion.

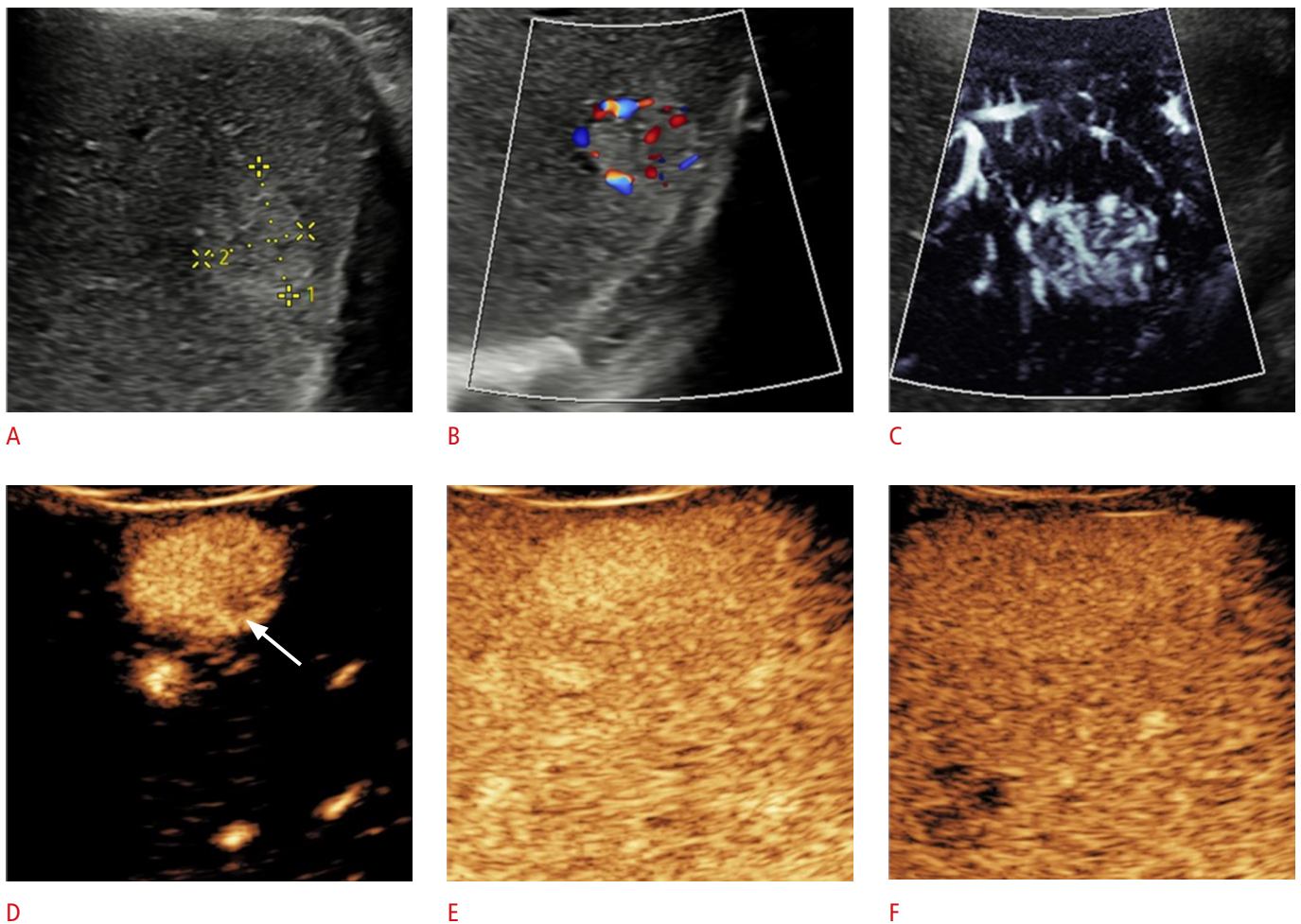


**Fig. 3.** A 33-year-old woman with focal nodular hyperplasia. Color Doppler, microvascular flow imaging (MVFI), and contrast-enhanced ultrasonography show a vascular pattern typical for focal nodular hyperplasia (patient 2). **A.** The patient had been treated for Crohn's disease, and a 26-mm, rounded, hyperechoic lesion was detected in segment VI of the liver with abdominal ultrasonography. **B.** A color Doppler image shows a non-specific, predominantly peripheral distribution of the signal. **C.** The lesion displays a spoke-wheel pattern with MVFI. The enhancement of the lesion is typical for focal nodular hyperplasia: after administration of an intravenous contrast agent, **(D)** the lesion enhances vividly in the arterial phase, and a hypoechoic central scar is also visible (arrow). **E, F.** The lesion shows sustained enhancement in the portal venous phase **(E)** and the delayed phase **(F)**.

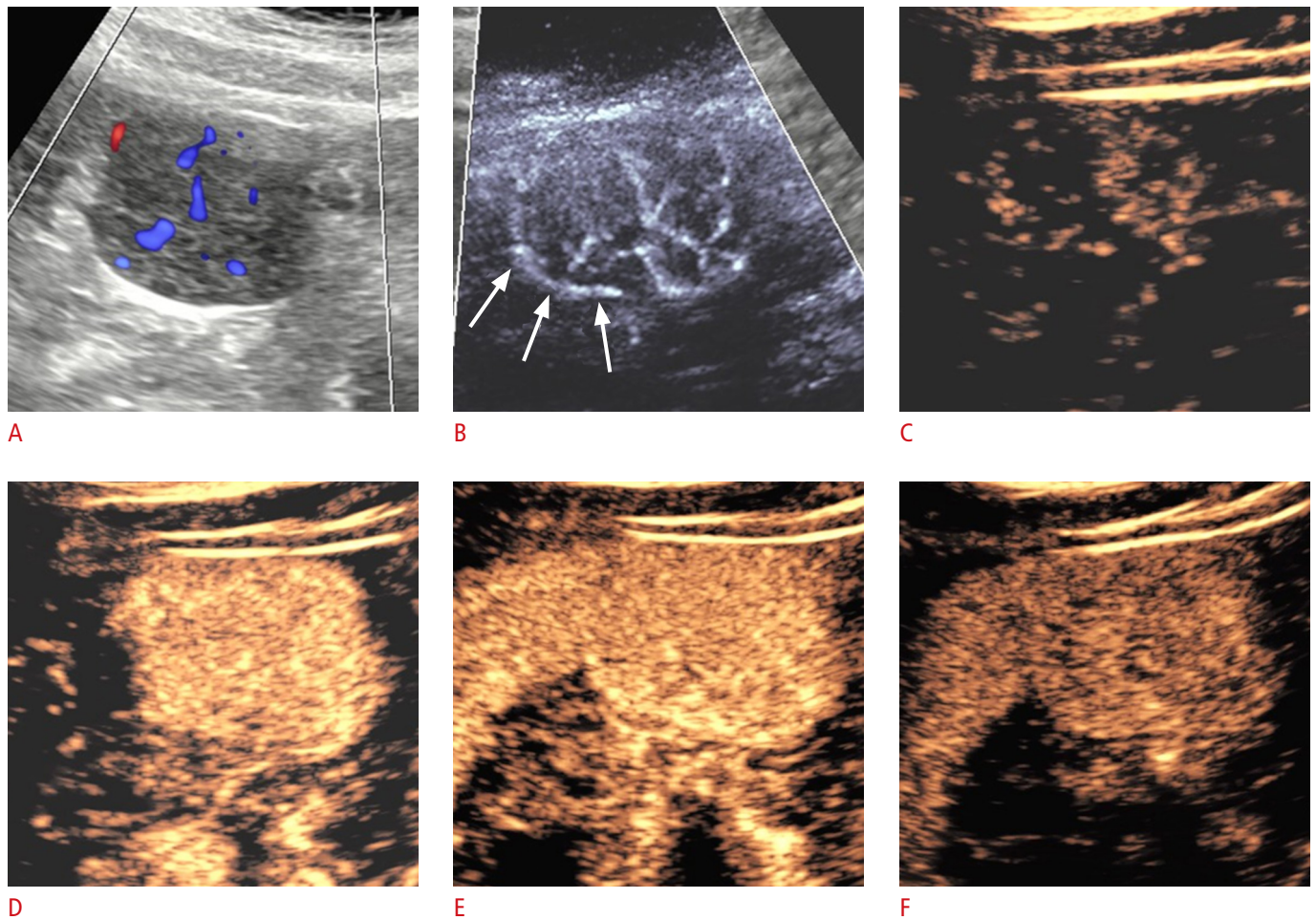


**Fig. 4.** A 43-year-old woman with focal nodular hyperplasia.

Color Doppler, microvascular flow imaging (MVFI), and contrast-enhanced ultrasound were used for the evaluation of the vascularity in a focal nodular hyperplasia (patient 3). A hypoechoic, well-circumscribed, 3.5-cm lesion is protruding from the edge of segment VI. **A.** The lesion is moderately vascularized on color Doppler ultrasonography. **B.** A spoke-wheel pattern is detected in the center of the lesion with MVFI. A draining vein forms a partial rim at the periphery of the lesion (arrows). **C.** A similar, wheel-shaped pattern consisting of arterioles radiating from a central feeding artery is detected during wash-in of intravenous contrast, a finding typical of focal nodular hyperplasia. **D–F.** The lesion is uniformly hypervascular in the arterial phase (**D**) and isovascular compared to the liver in the portal venous (**E**) and the late phases (**F**).

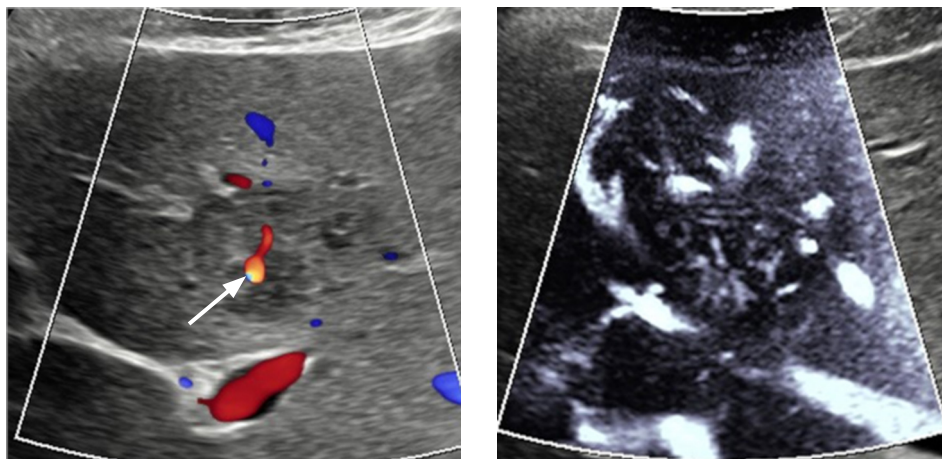
conventional Doppler technique has low sensitivity to slow-velocity flow. During CEUS, FNH appears as a highly vascular lesion showing arterial hyperenhancement (Figs. 3–5) and sustained contrast enhancement without washout in the portal venous (Figs. 3, 4), and delayed sinusoidal phases (Figs. 3, 4). In the very early arterial phase during wash-in of the contrast, a central feeding artery and centrifugal filling of arterioles arranged in a spoke-wheel pattern are also observed in typical cases (Fig. 5) [12]. A central scar is usually hypoenhancing in all phases (Fig. 3), and it is most frequently seen in lesions larger than 3 cm. In the present case series, the microvascular imaging pattern detected with MVFI was identical to the spoke-wheel distribution (Fig. 2) seen during the wash-in phase

with CEUS (Fig. 3), and it was consistently detectable even in small lesions (Fig. 5). Delicate hepatic veins draining the arterial in-flow can be visualized with MVFI (Fig. 4) at the lesion's periphery [13]. It is important to remember that central fibrosis and spoke-wheel vascularity are also imaging features of scirrhous-type HCC, which should be included in the differential diagnosis [14].

### MVFI Findings of Other Common FLLs

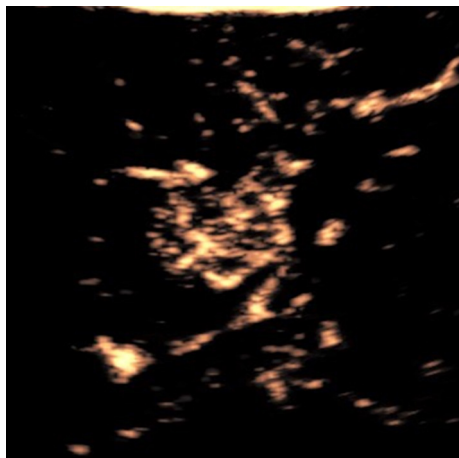
#### Hemangiomas

Hemangiomas are the most common non-cystic FLLs, with a prevalence of up to 20% in autopsy series [15]. A vast majority of

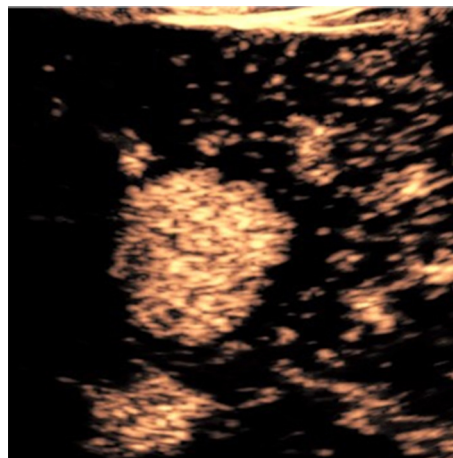


A

B



C

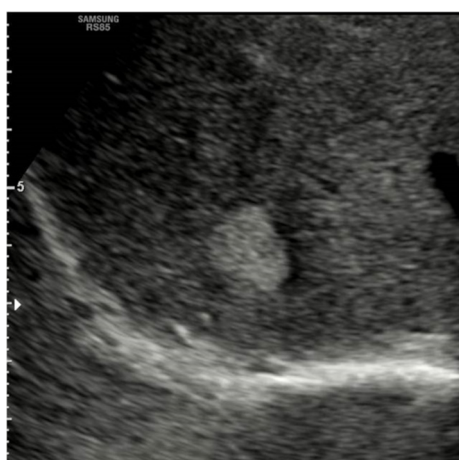


D

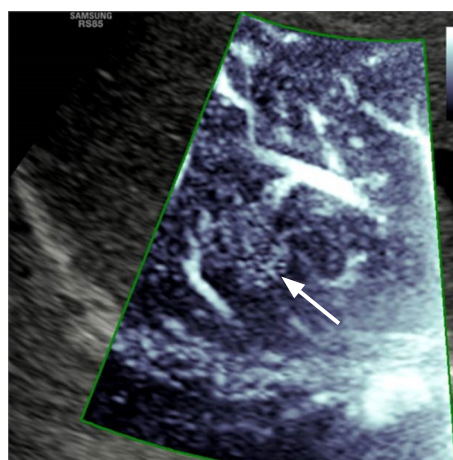
**Fig. 5.** A 23-year-old woman with focal nodular hyperplasia.

The vascularity was assessed with Color Doppler, microvascular flow imaging (MVFI), and contrast-enhanced ultrasonography in a focal nodular hyperplasia (patient 4). In a patient with a history of psoriasis, a 3-cm nearly isoechoic focal lesion was incidentally detected in segment IV.

**A.** A central arterial signal is visible with color Doppler ultrasonography (arrow). **B.** MVFI shows a delicate spoke-wheel pattern inside the lesion. **C.** Similar spoke-wheel vascularity is detected in the wash-in phase of contrast-enhanced ultrasonography. **D.** The lesion shows homogenous arterial hyperenhancement without washout of contrast in the delayed phase (images not shown) in keeping with the diagnosis of focal nodular hyperplasia.



A



B

**Fig. 6.** A 30-year-old woman with hyperechoic hemangioma.

Microvascular flow imaging (MVFI), assessment of the vascular pattern is shown in a hemangioma (patient 5). **A.** An oval, 2-cm, hyperechoic hemangioma is visible in segment VII with B-mode ultrasonography **B.** With MVFI, the lesion displays a dotted hypervascular pattern (arrow). The diagnosis of hemangioma was confirmed based on typical ultrasonography appearance and stability on follow-up scans.

hemangiomas are benign congenital malformations of mesenchymal origin. Histologically, cavernous hemangiomas are blood-filled cavities covered with endothelial lining encased in delicate

fibrous scaffolds. On B-mode US, hemangiomas are typically well-circumscribed hyperechoic lesions. Hemangiomas can be hypoechoic when the liver parenchyma is hyperechoic due to steatosis [10,16].

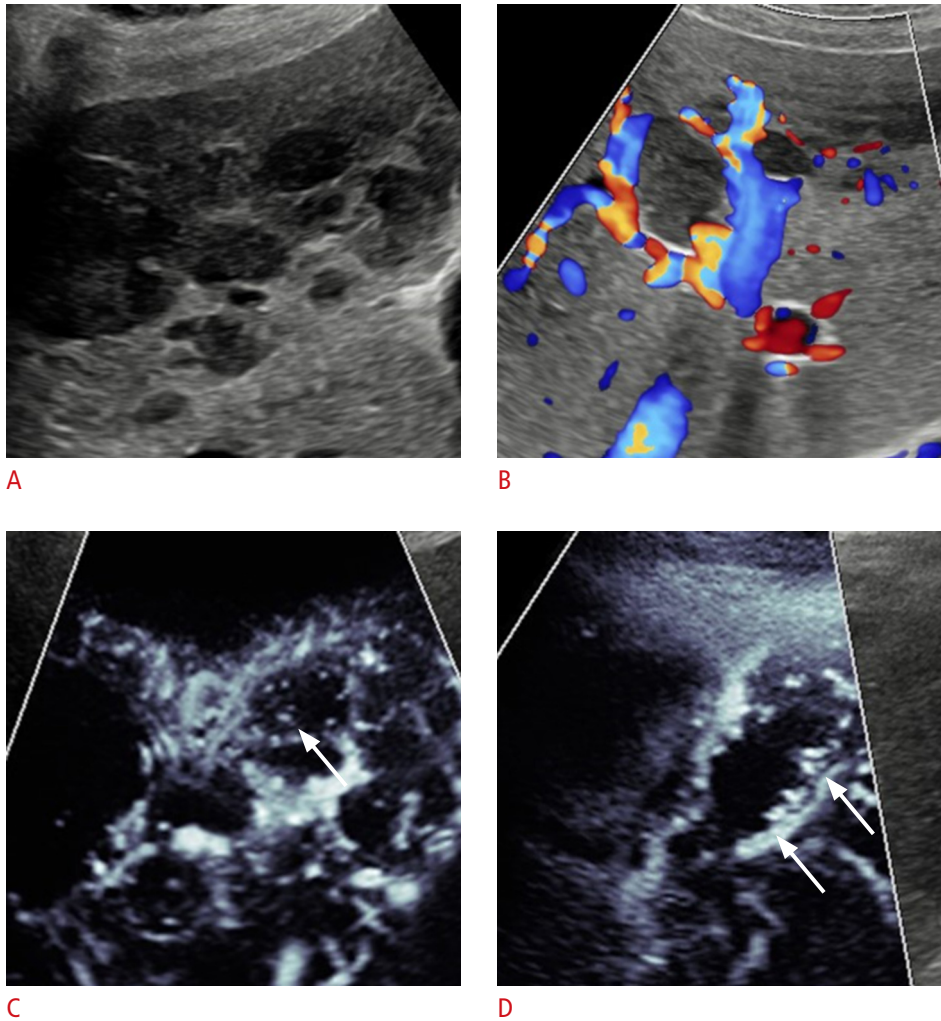


**Fig. 7.** A 70-year-old man with hepatic hemangiomas.

Color Doppler and microvascular flow imaging (MVFI) assessment of the vascularity is shown in a hemangioma (patient 6). **A.** A hypo-echoic, 8-cm-diameter lesion with a lobulated contour was detected with B-mode ultrasonography in the right lobe of the liver in a patient examined for suspected prostate cancer metastasis. **B.** Color Doppler ultrasonography shows a strong peripheral signal. **C, D.** A spotty dot-like pattern (**C**) and a nodular rim with a dot-like pattern (**D**) are detected inside the lesion with MVFI (arrows). The diagnosis of hepatic hemangiomas was confirmed with contrast-enhanced magnetic resonance imaging (images not shown).

Otherwise, CDI has limited value in characterizing cavernous hemangiomas, as most of these do not show internal Doppler signals. The capillary subtype typically consists of small, hypoechoic lesions and shows vascularity with CDI. High-flow lesions are frequently associated with arterioportal shunts and hypervascularity with CDI; they may cause hepatofugal portal venous flow in the neighboring parenchyma. Vascularity can be spotted in approximately two-thirds of hemangiomas with MVFI [8], although lesions smaller than 2 cm or located deep in the parenchyma are less likely to show a flow signal. A strip rim, a nodular rim, and a dot-like pattern are the most common vascular patterns detected in hemangiomas. A spotty dot-like pattern is more frequent in small lesions (Fig. 6), while a nodular rim with a dot-like pattern is predominant in larger lesions (Fig. 7). In hemangiomas, confluent cavernous lesions replace large parts of the liver. This lesion is often difficult to diagnose with B-mode US because of the poorly demarcated contours and heterogeneous echotexture.

Meanwhile, MVFI facilitates the diagnosis by revealing a cavernous hemangioma-like vascularity pattern (Fig. 7).

### Metastases

Metastases are the most common malignant liver lesions, most often originating from the gastrointestinal tract, breast, and lung. Therefore, differentiation from other FLLs is crucial. B-mode US has a high spatial resolution to find lesions even less than 1 cm in size, which makes it an excellent modality to demonstrate the multiplicity of lesions, a sign suggestive of metastatic disease. The echotexture of metastases is variable in grayscale images. However, features such as a round shape, a low echogenicity halo, or cystic areas due to necrosis are often indicative of metastasis. The CDI, due to its low sensitivity to small-caliber tumor vessels, has limited value in establishing the differential diagnosis [4]. Meanwhile, PDI has been reported to be superior to both CDI and contrast-enhanced CT for depicting the vascularity of metastatic adenocarcinomas. With MVFI,



**Fig. 8.** An 80-year-old woman with metastatic colorectal adenocarcinoma.

Microvascular flow imaging (MVFI) shows sparse vascularity in metastatic colorectal adenocarcinoma (patient 7). **A.** Multiple hyperechoic masses are visible with B-mode ultrasonography in the right lobe of the liver in a patient recently diagnosed with colon cancer. **B.** The mass has a hypovascular center and a vascular rim with MVFI. **C.** Contrast-enhanced computed tomography shows multiple hypodense lesions with peripheral rim enhancement. The diagnosis of metastatic colorectal adenocarcinoma was confirmed with a biopsy.



**Fig. 9.** A 69-year-old woman with metastatic pulmonary adenocarcinoma.

Power Doppler imaging (PDI) and microvascular flow imaging (MVFI) show abundant vascularity in a metastatic pulmonary adenocarcinoma (patient 8). **A.** In a patient with a history of pulmonary adenocarcinoma, a 3 cm, round, slightly hyperechoic mass with a hypoechoic halo was detected in segment IV. **B.** Color-coded PDI shows a weak signal at the periphery and in the center of the lesion. **C.** During MVFI, a high-signal rim and internal linear signals form a basket weave pattern (arrow), indicative of a hypervascular lesion. The diagnosis of metastatic lung adenocarcinoma was confirmed with a liver biopsy.

metastatic lesions typically display a hypervascular rim and variable grade and distribution of internal vascularity [6]. The majority of hepatic metastases, in particular lesions originating from colorectal and breast adenocarcinomas, are hypovascular and do not show an internal signal with MVFI (Fig. 8); while other, more hypervascular types of metastases can display non-specific distributions of internal vascularity (Fig. 9).

### Hepatocellular Carcinoma

HCC is the most common primary liver malignancy worldwide. Liver US is used for the surveillance of high-risk patients with cirrhosis to detect HCC. There is a significant overlap between the US features of HCC and other FLLs, although signs of fibrosis should raise the suspicion of HCC in case of any newly diagnosed FLL [10]. The US diagnosis can be more difficult for small HCCs, which can have a similar US appearance to regenerative nodules. Meanwhile, larger tumors are often heterogeneous and contain hyperechoic



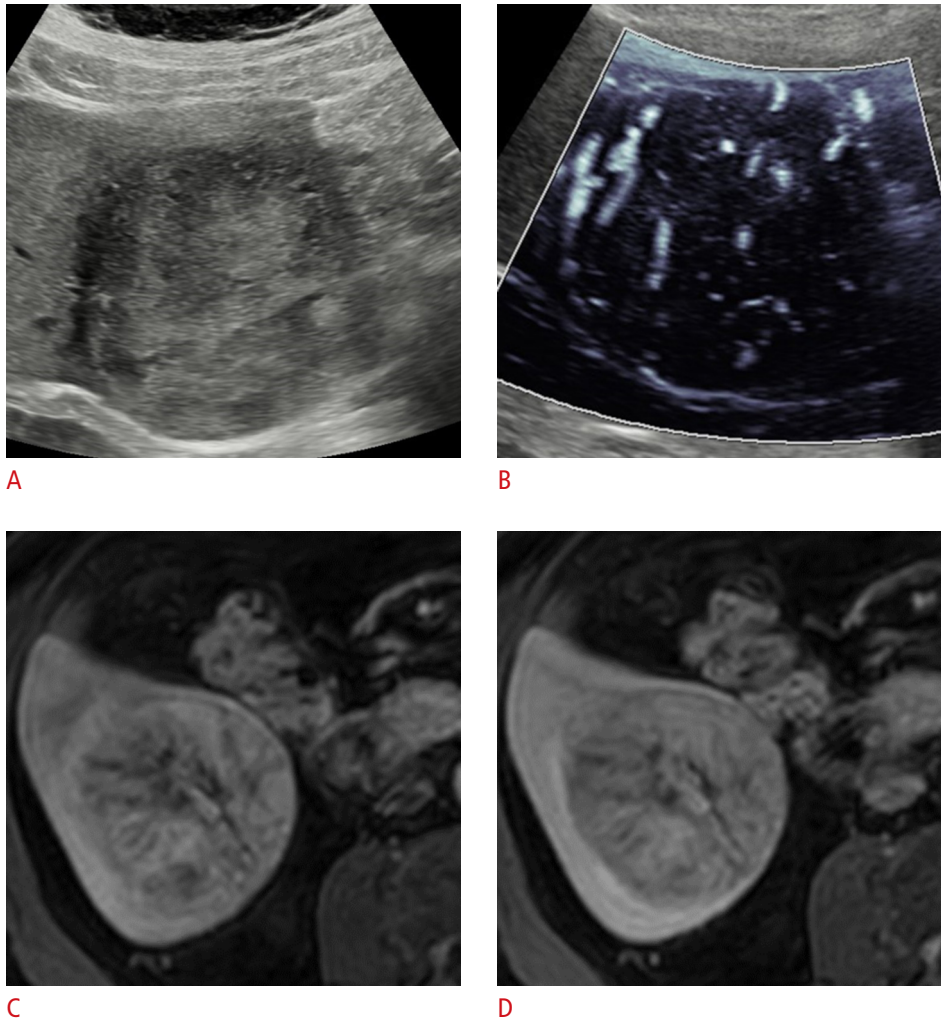


**Fig. 10.** A 78-year-old man with hepatocellular carcinoma.

Microvascular flow imaging (MVFI) assessment of the vascularity is shown in a hepatocellular carcinoma (patient 9). **A.** The patient had been investigated for non-alcoholic steato-hepatitis, and a 7-cm, solitary, mixed-echogenicity lesion with a hypoechoic capsule was detected in segment VI. **B.** The mass shows a non-specific dotted and linear hypervascular pattern with MVFI. The diagnosis of hepatocellular carcinoma is established with contrast-enhanced magnetic resonance imaging based on **(C)** arterial phase hyperenhancement and **(D)** portal venous phase washout. The diagnosis was also confirmed with a biopsy.

fatty and hypoechoic necrotic areas arranged in a mosaic pattern (Fig. 10). HCCs can show both peripheral and internal vascularity with CDI [4]. A lesion with an internal arterial signal is considered highly suspicious for HCC. MVFI can help to diagnose HCCs since it outperforms the sensitivity of detecting internal arteries in all other Doppler techniques [17]. However, the MVFI signal becomes less detectable with increasing depth and decreasing size; thus, contrast-enhanced examinations cannot be omitted from the work-up of HCC. The characteristic CEUS features of HCCs are intense early enhancement and progressive washout in the portal venous and delayed phases. Most HCCs are hypervascular due to their rich arterial supply (Fig. 10); thus, semi-quantitative grading of tumor vascularity in MVFI images can differentiate HCCs from non-HCCs with good accuracy. The common patterns detected with MVFI in HCC include the basket weave pattern [17], a combination of internal linear signals and a hypervascular rim, and the honeycomb pattern when signal-rich membranes encircle areas void of a signal [9].

## Conclusion

The advantages of MVFI are its ability to visualize low-velocity flow and its high spatial resolution, enabling the analysis of the microvessel architecture of FLLs. Similar to the wash-in phase with CEUS, a spoke-wheel distribution of microvessels is a typical finding that is consistently detectable in FNH using MVFI, even in small lesions. Vascular information obtained using MVFI can help characterize and distinguish FLLs.

ORCID: Aladár Dávid Rónaszéki: <https://orcid.org/0000-0002-2278-0058>; Ibolyka Dudás: <https://orcid.org/0000-0001-6488-8844>; Boglárka Zsély: <https://orcid.org/0000-0003-3163-886X>; Bettina Katalin Budai: <https://orcid.org/0000-0002-3982-7887>; Róbert Stollmayer: <https://orcid.org/0000-0003-4673-7588>; Oszkár Háhn: <https://orcid.org/0000-0002-2127-9181>; Barbara Csongrády: <https://orcid.org/0000-0001-7757-6495>; Byung-so Park: <https://orcid.org/0000-0001-6696-9437>; Pál Maurovich Horvat: <https://orcid.org/0000-0003-0885-736X>; Gabriella Györi: <https://orcid.org/0000-0001-9245-1287>; Pál Novák Kaposi: <https://orcid.org/0000-0002-7150-3495>

### Author Contributions

Conceptualization: Rónaszéki AD, Zsély B, Hahn O, Park BS, Maurovich-Horvat P, Györi G, Kaposi PN. Data acquisition: Rónaszéki AD, Dudás I, Zsély B, Györi G, Kaposi PN. Data analysis or interpretation: Rónaszéki AD, Zsély B, Budai BK, Stollmayer R, Csongrády B, Maurovich-Horvat P, Györi G, Kaposi PN. Drafting of the manuscript: Rónaszéki AD, Zsély B, Stollmayer R, Park BS, Györi G, Kaposi PN. Critical revision of the manuscript: Rónaszéki AD, Dudás I, Zsély B, Budai BK, Hahn O, Csongrády B, Maurovich-Horvat P, Kaposi PN. Approval of the final version of the manuscript: all authors.

### Conflict of Interest

The authors received no specific funding for this work. Pál Novák Kaposi has served as a speaker for Samsung Medison Ltd. All other authors declare no conflict of interest.

### Acknowledgments

We would like to thank Ms. Rita Tornai for assistance with ultrasound examinations and Ms. Vilma Kis for assistance with patient scheduling.

## References

1. Stollmayer R, Budai BK, Toth A, Kalina I, Hartmann E, Szoldan P, et al. Diagnosis of focal liver lesions with deep learning-based multi-channel analysis of hepatocyte-specific contrast-enhanced magnetic resonance imaging. *World J Gastroenterol* 2021;27:5978-5988.
2. Gore RM, Pickhardt PJ, Morteale KJ, Fishman EK, Horowitz JM, Fimmel CJ, et al. Management of incidental liver lesions on CT: a white paper of the ACR Incidental Findings Committee. *J Am Coll Radiol* 2017;14:1429-1437.
3. Matos AP, Velloni F, Ramalho M, AlObaidy M, Rajapaksha A, Semelka RC. Focal liver lesions: practical magnetic resonance imaging approach. *World J Hepatol* 2015;7:1987-2008.
4. D'Onofrio M, Crosara S, De Robertis R, Canestrini S, Mucelli RP. Contrast-enhanced ultrasound of focal liver lesions. *AJR Am J Roentgenol* 2015;205:W56-W66.
5. Lee DH, Lee JY, Han JK. Superb microvascular imaging technology for ultrasound examinations: Initial experiences for hepatic tumors. *Eur J Radiol* 2016;85:2090-2095.
6. Kang HJ, Lee JM, Jeon SK, Ryu H, Yoo J, Lee JK, et al. Microvascular flow imaging of residual or recurrent hepatocellular carcinoma after transarterial chemoembolization: comparison with color/power Doppler imaging. *Korean J Radiol* 2019;20:1114-1123.
7. Jeon SK, Lee JY, Han JK. Superb microvascular imaging technology of ultrasound examinations for the evaluation of tumor vascularity in hepatic hemangiomas. *Ultrasonography* 2021;40:538-545.
8. Wu L, Yen HH, Soon MS. Spoke-wheel sign of focal nodular hyperplasia revealed by superb micro-vascular ultrasound imaging. *QJM* 2015;108:669-670.
9. Yang F, Zhao J, Liu C, Mao Y, Mu J, Wei X, et al. Superb microvascular imaging technique in depicting vascularity in focal liver lesions: more hypervascular supply patterns were depicted in hepatocellular carcinoma. *Cancer Imaging* 2019;19:92.
10. Harvey CJ, Albrecht T. Ultrasound of focal liver lesions. *Eur Radiol* 2001;11:1578-1593.
11. Hosten N, Puls R, Bechstein WO, Felix R. Focal liver lesions: Doppler ultrasound. *Eur Radiol* 1999;9:428-435.
12. Yen YH, Wang JH, Lu SN, Chen TY, Changchien CS, Chen CH, et al. Contrast-enhanced ultrasonographic spoke-wheel sign in hepatic focal nodular hyperplasia. *Eur J Radiol* 2006;60:439-444.
13. Naganuma H, Ishida H, Ogawa M, Suzuki K. Visualization of draining vein in focal nodular hyperplasia by superb microvascular imaging: report of two cases. *J Med Ultrason (2001)* 2017;44:323-328.
14. Kim SH, Lim HK, Lee WJ, Choi D, Park CK. Scirrhous hepatocellular carcinoma: comparison with usual hepatocellular carcinoma based on CT-pathologic features and long-term results after curative resection. *Eur J Radiol* 2009;69:123-130.
15. Trotter JF, Everson GT. Benign focal lesions of the liver. *Clin Liver Dis* 2001;5:17-42.
16. Klotz T, Montoriol PF, Da Ines D, Petitcolin V, Joubert-Zakeyh J, Garcier JM. Hepatic haemangioma: common and uncommon imaging features. *Diagn Interv Imaging* 2013;94:849-859.
17. Bae JS, Lee JM, Jeon SK, Jang S. Comparison of MicroFlow Imaging with color and power Doppler imaging for detecting and characterizing blood flow signals in hepatocellular carcinoma. *Ultrasonography* 2020;39:85-93.